

UGe₂: A ferromagnetic spin-triplet superconductor

Andrew Huxley, Ilya Sheikin, Eric Ressouche, Nolwenn Kernavanois, Daniel Braithwaite, Roberto Calemczuk, and Jacques Flouquet

Département de Recherche Fondamentale sur la matière condensée, SPSMS, CEA-Grenoble, Grenoble 38054, France

(Received 24 July 2000; revised manuscript received 1 November 2000; published 22 March 2001)

The identification of a spin-triplet superfluid phase in ³He naturally led to more general theoretical predictions that spin triplet superconductivity might occur near to a ferromagnetic instability in some metals. The recent discovery of superconductivity near a ferromagnetic quantum critical point in UGe₂ now calls for these predictions to be reexamined experimentally. In this light it initially appears surprising that superconductivity in UGe₂ has only been detected in the ferromagnetic phase and not also at pressures above the critical pressure for the suppression of ferromagnetism. In this paper we provide evidence that the superconductivity is indeed a bulk property. We also observe the evolution with pressure of the magnetic order by neutron scattering and find that the ferromagnetic component of the order is still present at a pressure and temperature where superconductivity is found. In resistivity measurements we identify an additional transition within the ferromagnetic state. The characteristic temperature of this transition, T_x , decreases with pressure and disappears at a pressure P_x close to the pressure at which the superconductivity is strongest. Evidence is presented that this transition is also induced by a magnetic field at pressures just above P_x . An observed unusual reentrant behavior of the superconductivity with field at a pressure of 13.5 kbar is then qualitatively explained. These results suggest that the transition at P_x is intricately related to the appearance of superconductivity, which could explain why the superconductivity is apparently confined to the ferromagnetic phase.

DOI: 10.1103/PhysRevB.63.144519

PACS number(s): 75.50.Cc, 74.70.Tx, 75.30.Kz

INTRODUCTION

The discovery of superconductivity in single crystals of UGe₂ under pressure was only recently announced.¹ The most sensational aspect of this discovery is that at the pressure where the superconductivity is strongest, the Curie temperature ($T_{\text{Curie}}=35$ K) is almost two orders of magnitude higher than the superconducting critical temperature ($T_{\text{sc}}=0.8$ K). Although ferromagnetism and superconductivity have been shown to exist in other systems, notably ErRh₄B₄,^{2,3} HoMo₆S₈,⁴ and ErNi₂B₂C,⁵ in those cases $T_{\text{Curie}} < T_{\text{sc}}$ and the two orders can be considered to be competing. For the case of ferromagnetic nuclear-spin order, which has also been observed⁶ to exist in the superconducting state of AuIn₂, the nuclear and electronic spin systems are only very weakly coupled. More recently the coexistence of ferromagnetism and superconductivity has been claimed to occur in the layered structure RuSr₂GdCu₂O₈ with $T_{\text{Curie}} > T_{\text{sc}}$.⁷ In this case the two states might occur in different structural layers and high-quality single crystals have not yet been studied.

The superconductivity in UGe₂ disappears above a pressure $P_c \approx 16$ kbar that coincides with the pressure at which the ferromagnetism is suppressed. This fact suggests that the superconductivity and ferromagnetic order are in fact cooperative phenomena in this compound. The general defining property of superconductivity is the existence of permanent macroscopic currents that act to screen any static magnetic fields. To be compatible with ferromagnetism, the superconductivity (even if it has odd parity) must therefore be spatially modulated (at least to the extent of the mixed state of a conventional superconductor in an applied field), even when

no external field is applied. In this article we report on a series of measurements that address the origin and nature of the superconductivity and magnetism in UGe₂.

The layout of the paper is as follows. After some general discussion of the structure and background physics of UGe₂ we give some brief details of the sample preparation. We then focus the discussion on the pressure temperature phase diagram. The presence of an additional phase line that lies entirely within the ferromagnetic phase is suggested by a strong anomaly seen in the resistivity at a temperature $T_x(P, H)$. We examine the compatibility of our data with the idea that this transition might be associated with the formation of a charge density or spin density wave. This naturally leads on to a discussion of our neutron study and of the pressure evolution of the magnetic order. This study reveals a change in the temperature dependence of the ferromagnetic component of the order at high pressure, and a possible small modification of the magnitude of the ordered moment in zero field at T_x . However, we find no direct evidence for a charge density or spin density wave. An additional important result is that at 13 kbar there is no significant change in the ferromagnetic component of the order ($1 \mu_B$ /uranium) on entering the superconducting state. Having established that the ferromagnetic order is present at the same pressure and temperature as the superconducting state, we then return to discuss the details of the latter. We summarize our measurements of the flux-flow resistivity, which are consistent with bulk superconductivity. In critical-field measurements we detected a very unusual reentrant behavior of the upper critical field at 13.5 kbar. This feature is clearly correlated with the transition at $T_x(P, H)$ which is induced by field at this pressure. The occurrence of superconductivity in UGe₂ thus appears to be intimately related to the transition at $T_x(P, H)$.

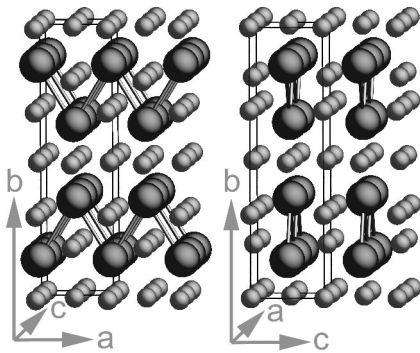


FIG. 1. The crystal structure of UGe_2 is shown. Thick bars connect nearest neighbor uranium atoms (large spheres) that form zigzag chains parallel to the crystal a axis (the easy magnetization direction). The Ge atoms are shown as small spheres and the orthorhombic unit cell by the fine lines.

GENERAL CONSIDERATIONS

We do not believe the superconductivity we see in the ferromagnetic state of UGe_2 to be an isolated event restricted to some special combination of circumstances. Rather we believe that odd-parity superconductivity can occur quite generally when ferromagnetic fluctuations are large enough, in the absence of competing orders, and when crystals can be made sufficiently pure to avoid the pair-breaking influence of defects.^{8,9} The values of the critical temperature found for UGe_2 and the fact that superconductivity is not detected in the paramagnetic phase above P_c might, however, be related to some special features of this material. It is then interesting to briefly review what the general distinguishing features of UGe_2 are.

First, the magnetic properties of UGe_2 are strongly anisotropic, which is a common trait of light-actinide compounds.¹⁰ The inherent anisotropy due to the uranium $5f$ electrons is further emphasized by the choice of an orthorhombic crystal structure (space group Cmmm).^{11,12} The uranium atoms are arranged as zigzag chains of nearest neighbors that run along the crystallographic a axis, which is the easy magnetization direction. The chains are stacked to form corrugated sheets as in alpha uranium but with Ge atoms included at interstitial positions. Additional planes of Ge atoms (Fig. 1) separate the sheets along the b axis. The similar unusual low-symmetry structure of alpha uranium is favored energetically since it splits the large density of states that would otherwise be present at the Fermi energy of more compact structures.^{13,14} A local minimum in the density of states at the Fermi energy for the orthorhombic structure might then be expected. The observation of a field-induced polarized state (metamagnetic behavior) above P_c (Ref. 15) in UGe_2 , gives convincing evidence that for UGe_2 there is indeed such a minimum. For uranium the orthorhombic cell is still prone to nesting,¹⁶ and alpha uranium exhibits a complex charge density wave (CDW) below 43 K.¹⁷ For UGe_2 , band structure calculations^{18,19} also suggest that there is a possible proximity to nesting which raises the possibility that a CDW might also appear. Since the Fermi surfaces are already split into majority and minority spin surfaces in the ferromagnetic phase, in this case a CDW almost automati-

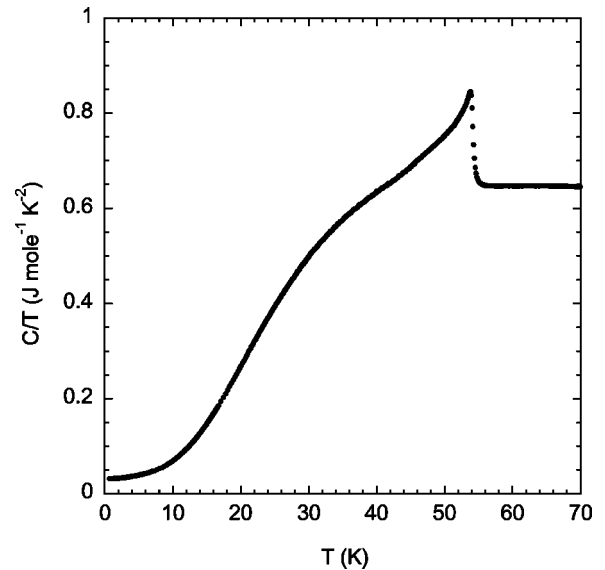


FIG. 2. The ambient-pressure specific heat divided by the temperature T is plotted against T . The convex form of the curve most probably indicates a substantial contribution from low-energy phonons or another soft mode. The height of the jump at the Curie temperature and low-temperature limiting value ($32 \text{ mJ mol}^{-1} \text{ K}^{-2}$) are discussed in the main text.

cally implies a spin density wave (SDW). In general, high pressures would favor the choice of a more symmetric cell and for uranium the CDW can be suppressed by application of pressure.²⁰

The important difference between UGe_2 and α -uranium is that in UGe_2 the nearest-neighbor uranium separation, $d_{\text{U-U}} = 3.85 \text{ \AA}$, is larger. The increased uranium separation leads to a greater localization of the f electrons²¹ and much larger magnetic entropy at low temperature. At ambient pressure, a degree of delocalization of the f electrons is, however, suggested²² by the moderate value of the low-temperature specific heat (Fig. 2), $C/T = 32 \text{ mJ mol}^{-1} \text{ K}^{-2}$, and the ratio of this to the step in C/T ($\approx 200 \text{ mJ mol}^{-1} \text{ K}^{-2}$) at T_{Curie} . The value of the ordered moment, $1.48\mu_{\text{B}}$ /uranium, which is less than half the value for an isolated uranium ion, $3.7\mu_{\text{B}}$, does not give unequivocal evidence about the extent of delocalization, since a reduction of this order can be potentially explained by crystal field splitting alone. The small value of the ordered moment compared to the Curie-Weiss moment ($2.8\mu_{\text{B}}$ /uranium) deduced from the susceptibility above T_{Curie} is, however, consistent with a weak delocalization.^{23,24} Pressure should increase the extent of delocalization of the f electrons as $d_{\text{U-U}}$ is decreased. This offers a possible mechanism to explain the suppression of the Curie temperature. Apart from separating the uranium atoms it should be remembered that the Ge atoms might also play a second role in hybridizing with the uranium ($d_{\text{U-Ge}} = 2.9 \text{ \AA}$). The susceptibility of UGe_2 is extremely anisotropic compared to α -uranium, which does not order magnetically and has a nearly isotropic susceptibility. Measurements at high fields reveal that the magnetic anisotropy energy in UGe_2 is indeed extremely large²⁵ and that the electron spins are thus expected to behave like Ising spins.

The importance for superconductivity of these observations is threefold: (i) the uniaxial nature of the magnetic anisotropy diminishes the magnitude of transverse magnetic fluctuations that would otherwise be pair breaking for a triplet (spin-parallel) paired superconducting state. (ii) A tendency toward nesting of the Fermi surface might enhance the coupling of the spin fluctuations with electronic excitations close to the pairing vector ($2k_f$) and therefore favor superconductivity. This condition might be expected to depend sensitively on the volumes enclosed by the majority and minority spin Fermi surfaces and therefore on the magnetization of the sample. (iii) The possible strong energy dependence of the electronic density of states at the Fermi level might actually reduce the effect of very low energy magnetic fluctuations. These fluctuations might be pair breaking rather than pair forming.²⁶

Finally, the one other essential fact relevant to the appearance of spin-triplet superconductivity is that UGe₂ is intrinsically structurally ordered. This and a favorable metallurgy mean high-quality crystals containing few defects can be made.²⁷ Non-*s*-wave superconductivity is expected only in very pure crystals since, contrary to the case for conventional isotropic *s*-wave superconductors, all defects are pair breaking.

CRYSTAL SYNTHESIS

The crystals used in the experiments reported here have ambient-pressure residual-resistance ratios of above 100 parallel to the *b* axis. They were grown from a zone-purified ingot by the Czochralski technique under a highly purified pressurized argon atmosphere. Radio-frequency heating and a cold crucible were used. The crystals were additionally annealed for 2 days under ultrahigh vacuum. Preliminary neutron diffraction studies suggest that the annealing may be important to remove stacking faults along the crystal *b* direction. Resolution-limited diffraction peaks (FWHM=0.3°) were recorded by neutron diffraction, and no change of the peak width was seen with applied pressure.

PHASE DIAGRAM AND T_x

The pressure-temperature phase diagram determined from resistivity and susceptibility measurements is shown in Fig. 3. The measurements performed in Grenoble were performed on two sections of the same single crystal. The resistivity was measured for a current applied along the *a* axis and the ac field was applied along the same axis in the susceptibility measurements. Also shown are measurements made at Cambridge (Saxena *et al.*¹) on single crystals and polycrystals cut from the polycrystalline zone-refined ingot. The superconducting transition is seen in both susceptibility and resistivity measurements. The existence of an additional phase transition, not shown in this figure, has been previously suggested in the literature,²⁸ although the evidence for it then appeared rather tenuous. An anomaly seen in the thermal expansion at ambient pressure,²⁹ might rather be related to a change in the pinning of magnetic domain walls, and therefore not relate directly to a thermodynamic transition. In magnetic measure-

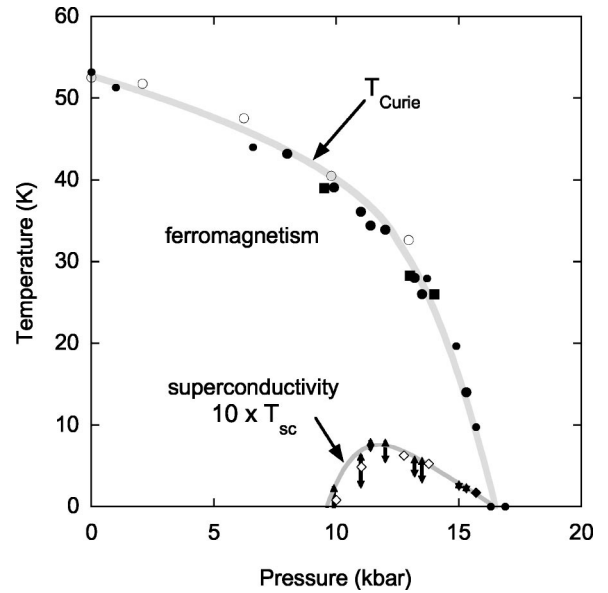


FIG. 3. The pressure-temperature phase diagram of UGe₂. The full symbols were measured in Grenoble on the same single crystal. The Curie temperature was taken as the temperature at which the ac susceptibility shows a sharp maximum (small circles) or as the temperature at which there is a discontinuity in the slope of the resistivity (large circles). The Curie temperatures determined by neutron scattering are shown by full squares. The onset temperatures for superconductivity and the temperatures at which the resistive transitions were complete are indicated by solid triangles joined by vertical lines. The point at 15.7 kbar (filled diamond) shows the onset determined by ac susceptibility at this pressure. The open symbols were determined on other crystals (see text) in Cambridge; the midpoint of the superconducting transition alone is given for these measurements. The lines are to guide the eye.

ments we see a large magnetic remanence and hysteresis below 10–30 K, depending on the measurement conditions, whereas there is almost no hysteresis closer to T_{Curie} . This behavior qualitatively resembles previous results for UCoGa.³⁰ In accord with previous studies,²⁵ we find no pronounced anomalies in the specific heat and resistivity at ambient pressure, other than at the Curie temperature (Fig. 2). The convex curvature of the specific heat visible below T_{Curie} could, however, indicate that there is an important contribution from low-energy phonons or other excitations, suggestive of a Kohn anomaly,³¹ and a proximity to nesting of the Fermi surface. We have not yet performed measurements of the specific heat under pressure. However, at pressures approaching 12 kbar we do see a second sharp change in the slope of the resistivity at a low temperature, $T_x(P)$, in addition to the change of slope at the much higher Curie temperature and superconductivity (Fig. 4). This feature becomes very weak at pressures lower than 10 kbar, but can tentatively be associated with the previously reported²⁸ broad peak in the derivative of the resistivity. This peak is centered at about 30 K when $P=0$, which corresponds approximately to the position of the broad feature in the specific heat. Above 13 kbar, the strong feature visible at 12 kbar is absent. A much weaker feature is, however, discernible at low temperature, that is more akin to a crossover or coherence tem-

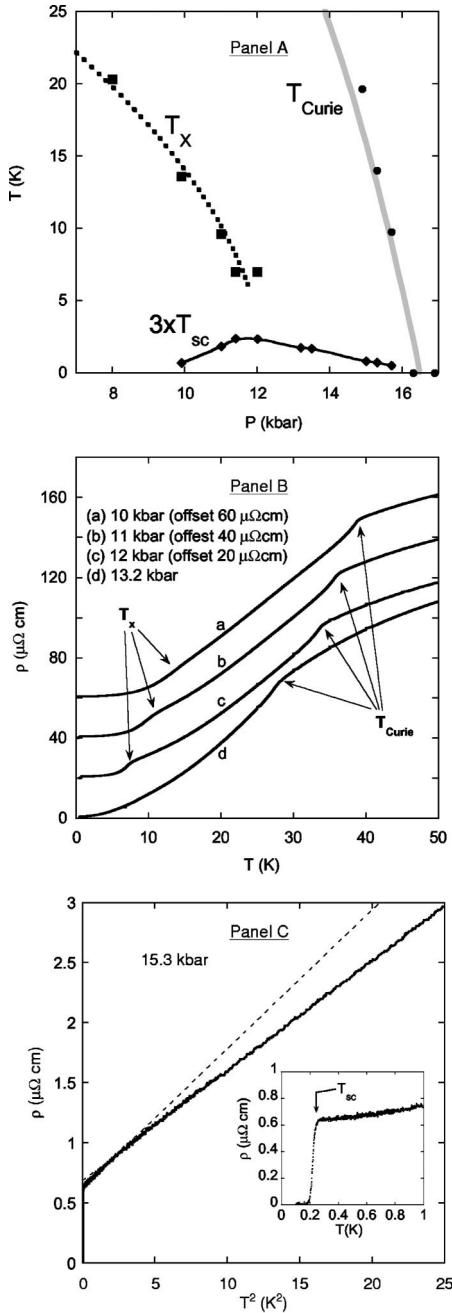


FIG. 4. Panel A shows the temperature T_x of an anomaly seen in the resistivity as a function of pressure (solid squares). The lines showing the onset of the superconducting transition and Curie temperature are also redrawn from Fig. 3. The anomaly at T_x occurs in addition to a change in slope of the resistivity at the Curie temperature and superconductivity. Resistance curves showing all three features at different pressures are shown in panel B. The anomaly at T_x becomes much less marked at low pressure, but a broad maximum in $d\rho/dT$ can still be identified (the small glitches at 5 K intervals are experimental artifacts). Above 13 kbar there is no strong feature corresponding to T_x . However, a small change in slope is apparent at low temperature when the resistivity is plotted against T^2 . This is illustrated by the resistance curve shown in panel C for a pressure of 15.3 kbar. The dashed lines are extensions of fits to $\rho = \rho_0 + AT^2$, above and below the region where the slope changes. The inset shows the superconducting transition at this pressure.

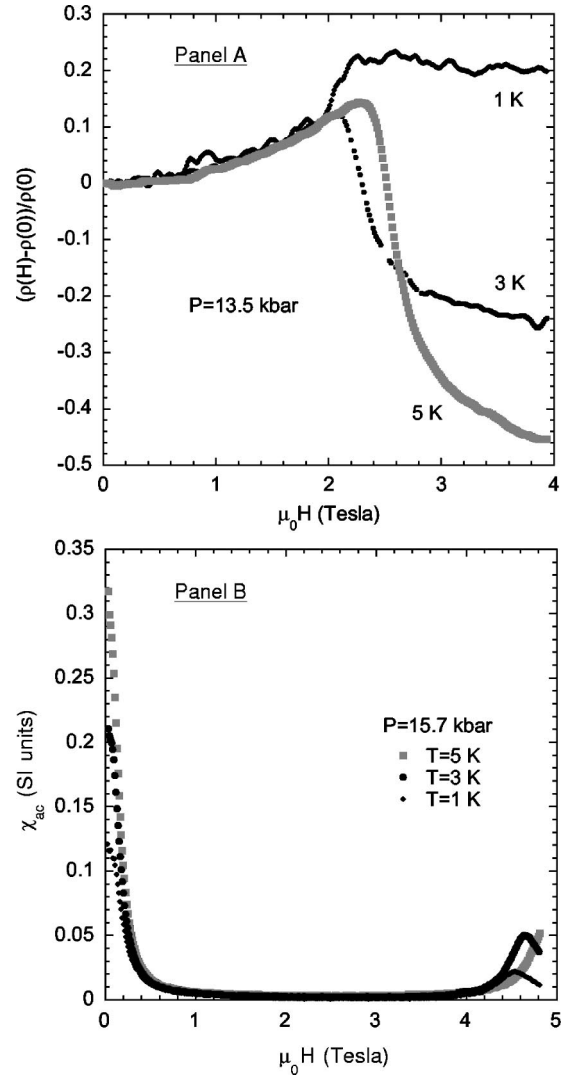


FIG. 5. Panel A shows the relative longitudinal magnetoresistivity measured at 13.5 kbar and different low temperatures in an increasing field. Panel B shows the ac susceptibility measured at 15.7 kbar. The field was applied parallel to the easy magnetization direction in both cases. The anomalies at 2 and 4.5 T occur in the ferromagnetic state for pressures greater than $P_x \approx 12.5$ kbar (see text).

perature and corresponds to a small change in the T^2 coefficient of the resistivity [Fig. 4(c)]. However, in this pressure range ($13 \text{ kbar} < P < P_c$) the low-temperature susceptibility and resistivity display a sharp anomaly in an applied magnetic field (Fig. 5). These anomalies occur at fields and pressures that are distinct from, and should not be confused with, the previously reported metamagnetic behavior¹⁵ seen at pressures above P_c . The present features, namely, a step in the resistivity and a peak in the ac susceptibility occur in the magnetically ordered state at a characteristic field that increases with pressure and extrapolates to zero near $P_x \approx 12.5$ kbar. The results suggest that magnetic field shifts the line $T_x(P)$ measured in zero field to higher pressure. This observation supports the view that T_x might correspond to a phase transition facilitated by a special geometry of the Fermi surfaces. The Fermi surfaces for the majority and mi-

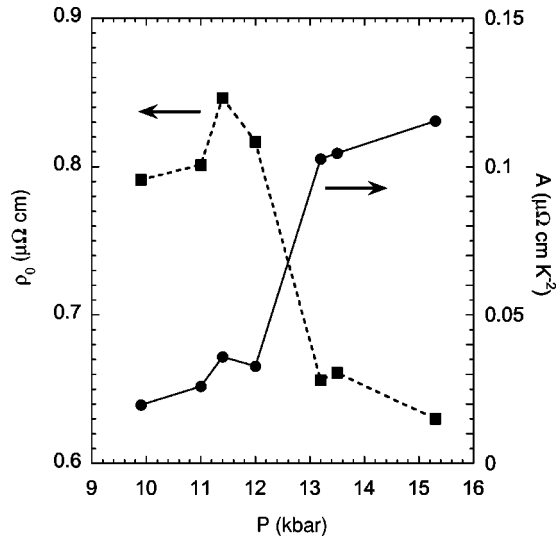


FIG. 6. At all the pressures examined, the low-temperature resistivity immediately above the superconducting transition is well described by $\rho = \rho_0 + AT^2$. The residual resistivity ρ_0 and the T^2 coefficient A are shown as a function of pressure. Other data³² show that the A coefficient falls at higher pressures above $P_c \approx 16$ kbar. The data are characterized by a sharp increase in A and fall in ρ_0 at the pressure P_x . The lines serve to connect the points.

nority spin directions are expected to expand and contract as the spin polarization is increased. A special condition, such as a nesting of the spin majority Fermi surface, might then be fulfilled when the splitting approaches a particular value. This could give rise to a phase line in the ferromagnetic state below $T_{\text{Curie}}(P)$ corresponding approximately to a constant value of the ordered ferromagnetic moment.

The microscopic nature of the transition remains elusive as discussed below. However, we can speculate that the critical slowing down of the fluctuations related to the transition could be the driving force for the superconducting pairing. This is supported by the fact that the superconductivity is strongest close to the pressure, $P_x \approx 12.5$ kbar, where T_x vanishes. Examination of the T^2 coefficient of the electrical resistivity further supports this hypothesis. It has previously been pointed out that the T^2 coefficient is apparently peaked at 12–13 kbar rather than at P_c .²⁸ We find that the T^2 coefficient (defined in the limit of low temperature) grows rapidly at 11 kbar and remains large over the range of pressures where superconductivity is seen (Fig. 6). Previous reports^{28,32,33} show that the T^2 coefficient decreases smoothly with pressure above P_c . A different law $\rho = \rho_0 + AT^n$ with $n < 2$ is usually found in other systems near a second-order quantum-critical point, but such a behavior would not be expected for UGe₂ near P_c if the transition is first order as we propose. In the ferromagnetic state we again find the Fermi-liquid exponent $n = 2$ even close to P_x . This indicates that spin waves, which might be expected to give $n > 2$ do not make a significant contribution to the resistivity. Further, if there is any deviation from the $n = 2$ exponent near the critical point at P_x , it must occur in a pressure interval sharper than the interval between our data points (1 kbar).

If we do indeed interpret the anomaly at T_x to be a signature of a phase transition, it is interesting to see how far we can go in explaining qualitatively some of the details of our observations. To be definite we will consider the scenario of a CDW/SDW transition. The effect on the resistivity of the CDW/SDW depends sensitively on the amplitude of the CDW/SDW, the angle of the current to the nesting vectors, as well as the magnitude of the nesting vectors, which determine the effectiveness of the CDW/SDW fluctuations in scattering the conduction electrons. For a 3D material all these quantities can evolve continuously with temperature and pressure (as for the CDW in alpha uranium). In the CDW/SDW phase the low-energy density of states is reduced due to the formation of a gap in nested regions of the affected Fermi surfaces. At low-enough temperature this would then lead to an increase in the resistivity, particularly for currents parallel to the CDW/SDW nesting vectors. From the calculated Fermi surfaces in UGe₂, nesting vectors close to the c axis appear to be the most likely, which would be perpendicular to the current in our measurements. However, in agreement with the above argument we still find that the residual resistivity of our sample is higher below P_x (Fig. 6). At higher temperature, fluctuations in the CDW/SDW might lead to an increase in scattering of the conduction electrons that is peaked at T_x , but disappears rapidly below T_x . The form of the resistivity we observe near T_x is broadly consistent with this effect acting in parallel with other scattering processes. A similar situation is found for our data in an applied field. Figure 5 shows that the resistivity falls on entering the high-field phase (the supposed CDW/SDW phase) at temperatures of several Kelvin and above, which corresponds to a reduction in the scattering of the conduction electrons in the CDW/SDW state. At lower temperature the situation is reversed and the resistivity increases abruptly on entering the CDW/SDW phase. At low temperature there are few thermally excited fluctuations and the scattering is due to sample defects or impurities. In this case the change of the resistivity is dominated by the opening of the gap and a reduction in the low-energy electronic density of states.

Although all the attributes of the charge density wave can change with pressure it still appears surprising^{34,35} that the anomaly in the resistivity weakens so rapidly with decreasing pressure below P_x whereas T_x increases. To develop this point further, we note that a nesting or near nesting of the Fermi surfaces alone is not sufficient to form a CDW/SDW structure. The interaction between electrons on the nested sheets must also be considered. It is possible that the spectrum of the magnetic excitations therefore plays a role in determining the amplitude of the CDW/SDW in conjunction with other excitations such as phonons. Since the low-temperature magnetic fluctuations are modified as P_c is approached, this could offer a scenario to explain an increase in amplitude of the CDW/SDW. Such an idea is not unprecedented, as the proximity to a magnetically ordered (antiferromagnetic) state has previously been suggested to underpin the formation of an SDW state in chromium.³⁶ We thus arrive at a picture in which the nesting condition is optimized for a particular splitting of the spin majority and minority

sheets corresponding to a ferromagnetic moment of about $1.2\mu_B$. For $P > P_x$, the ordered moment in zero field is smaller than this and the relevant Fermi surfaces are not close to fulfilling the nesting condition at any temperature. Below P_x the interaction that controls the amplitude of the CDW/SDW might depend in part on the magnetic fluctuations associated with P_c and these increase in amplitude as P approaches P_c . A full treatment of the problem should then include the coupling between the various order parameters, magnetic fluctuations, including other low energy (finite q) modes as well as those directly associated with the ferromagnetic order, and phonons. In the next sections we describe our neutron measurements. Although we do not find any direct evidence for a CDW/SDW our results do suggest that the ferromagnetic order is slightly modified by the transition at T_x .

CRYSTAL STRUCTURE

The crystal structure of our crystals was examined by neutron diffraction on the four-circle instrument D15 at the Institute Laue Langevin (ILL), France. Approximately 150 independent reflections were measured for two incident wavelengths (0.85 and 1.17 Å). A refinement of the previously published structure^{11,12} (space group no. 65, Cmmm) accounted for the data with a weighted deviation of $R = 5.25\%$ and $\chi^2 = 3.08$.

MAGNETIC STRUCTURE AT AMBIENT PRESSURE

The change in the temperature dependence of the resistivity with pressure suggests that the low-temperature magnetic structure might change at about $P_x = 12.5$ kbar. This motivated us to study the magnetic structure more closely by neutron diffraction with the D23 instrument at the ILL. A complete study at atmospheric pressure³⁷ with polarized neutrons revealed that the magnetization density is due to uranium f moments with a low-temperature (5 K) moment of $M_{U-5f} = 1.48(2) \mu_B/\text{uranium}$ (at 4.7 T) with no contribution from the Ge sites ($M_{Ge-3d} < 0.01 \mu_B$). The best fit to the form factor is obtained for either a U^{4+} ion with a reduced $5f$ orbital contribution ($\mu_L/\mu_S = -2.60$) compared to an isolated ion ($\mu_L/\mu_S = -3.34$), or alternatively to a U^{3+} ion with close to a full orbital contribution. From the neutron scattering it is not possible to distinguish between these two scenarios. For comparison, the orbital contribution is completely absent for alpha uranium (with U^{3+}),³⁸ which has no local moments and a strongly delocalized f band, whereas the full orbital contribution characteristic of an isolated U^{4+} ion is found for the compound UO_2 . The case for UGe_2 is intermediate, again indicative of a weak delocalization of the f electrons.³⁹ The profile of the form factor was found to be unchanged in the paramagnetic state at 60 K (4.7 T), and at an intermediate temperature of 30 K. Direct measurement of the saturation moment in a SQUID magnetometer gave $M_{\max} = 1.50(2) \mu_B/\text{uranium}$ (also at 4.7 T and 5 K), with no significant field dependence at this field. Any contribution from the polarization of the uranium $6d$ orbits must therefore be almost exactly compensated by an opposite polarization

from other non- f conduction bands. Finally, a complementary study by x-ray magnetic circular dichroism³⁷ supports the choice of a U^{4+} form factor over U^{3+} .

NEUTRON SCATTERING UNDER PRESSURE

Due to the near cancellation of the nuclear scattering lengths at some magnetic peak positions, it is straightforward to measure the magnetic moment as a function of temperature at different pressures without resorting to polarized neutrons. The 001 peak is particularly suited to study since the magnetic structure factor is large at small wave-vector transfer, while this peak has only a small nuclear contribution. The integrated intensity of this peak therefore gives a direct measurement of M_f^2 .

The experiments under pressure were made with the ILL piston-cylinder pressure cell on the D23 instrument. Cylindrical crystals of height 2 mm parallel to the b axis, and diameter 2 mm, cut from the same parent crystal as the samples used to determine the phase diagram were used. The samples were mounted vertically on a single crystal of NaCl and held at the center of a sealed copper capsule of internal diameter 3 mm containing the pressure-transmitting medium (a deuterated ethanol/methanol mixture). The construction of the pressure cell restricts the incident and diffracted beams to lie within a narrow angular window of $\pm 6^\circ$ to the horizontal plane. To be sure not to truncate peaks we only considered peaks inclined within $\pm 4^\circ$. The pressure was estimated by determining the change in lattice parameter of the NaCl.

Although Friedel pairs of peaks gave equal intensities within 10%, the ratios of the various strong nuclear-peak intensities differed by up to 50% from their calculated values. This reflects an angular dependence of the absorption and scattering from the cell body. The intensity from the strong nuclear peaks, however, did not evolve with pressure. We therefore measured the accessible peaks at zero pressure and low temperature and normalized the data at other pressures (9.5 and 13 kbar) to the zero-pressure values. The data at 14 kbar were measured at a different time with another crystal and a different configuration of the spectrometer. The analysis of the data at 14 kbar is therefore limited to presenting the temperature dependence of the scattering of the magnetic 001 peak. This data has been normalized to the 002 Bragg peak to place it on the same scale as the other measurements, although it should be remembered that the absolute value of M_f^2 deduced for this pressure might not be accurate.

EVOLUTION OF THE CRYSTAL STRUCTURE WITH PRESSURE

Although the intensity of the strong nuclear peaks did not change, the intensity of the weak nuclear peaks of type $\langle 310 \rangle$ and $\langle 312 \rangle$ decreased slightly with pressure. This is shown in Fig. 7. The decrease can be explained by a small displacement of the atoms. The structure factors for the 310 and 312 peaks are the same,

$$f = 4f_U \cos(2\pi y_U) + 4f_{Ge} \cos(2\pi y_{Ge}) \\ \Rightarrow f = (0.96 - 19.2 \times \delta y_{Ge} - 16.4 \times \delta y_U) \times (10^{-12} \text{ cm}),$$

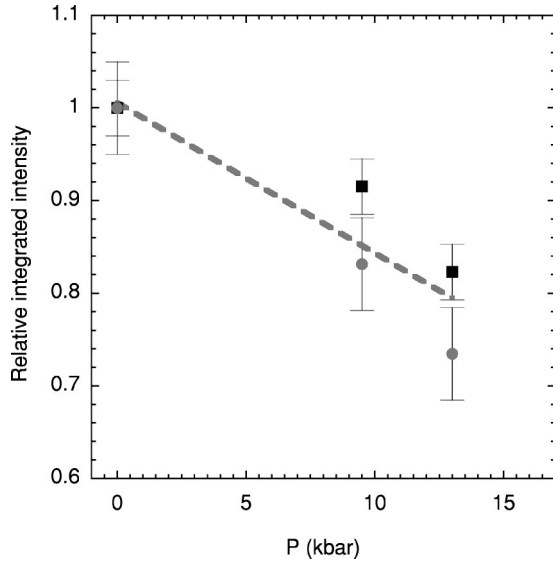


FIG. 7. The integrated intensities of the $\langle 312 \rangle$ (squares) and $\langle 310 \rangle$ (circles) diffraction peaks normalized to their ambient-pressure values are shown as a function of pressure. The measurements shown were made at low temperature, but no significant temperature dependence of the diffracted intensities was observed up to 60 K. The peaks are therefore nuclear in origin, and for the Cmmm structure should have an identical structure factor. The observed reduction in intensity with pressure is consistent with a flattening of the corrugations of the uranium nearest-neighbor chains. The line serves only to guide the eye.

where δy_U and δy_{Ge} are the displacements of the uranium and Ge1 atoms in the unit cell from their zero-pressure values of 0.141 and 0.308 (measured in units of the unit-cell parameter $b = 15.04 \text{ \AA}$). The decrease in the intensity of the $\langle 312 \rangle$ and $\langle 310 \rangle$ peaks is consistent with a small increase in either or both of δy_{Ge} and δy_U of the order $10^{-3} \text{ kbar}^{-1}$. This corresponds to a straightening of the buckled uranium chains with applied pressure. This would be consistent with a larger compressibility along the b direction compared to the other directions. Although the compressibility κ has not been directly measured, the Grüneisen relation ($\kappa = 3V\alpha/\Gamma C$, where Γ is a constant, C is the specific heat, and α is the thermal expansion) suggests that the thermal expansion should also be largest along the b direction above T_{Curie} . This indeed appears to be the case,²⁹ although the anisotropy of α is not very large. The magnitude of the jump in the thermal expansion coefficient at T_{Curie} is, however, almost a factor of 2 larger parallel to the b direction than for the c direction, both directions being perpendicular to the ordered moment.

TEMPERATURE AND PRESSURE DEPENDENCE OF THE MAGNETIZATION

Figure 8 shows the temperature evolution of M_f^2 measured at various pressures. The minimum value of the moment detectable is $0.1\mu_B$, against background scattering from the cell, a weak nuclear contribution to the 001 peak and a weak contribution due to $\lambda/2$ contamination from the

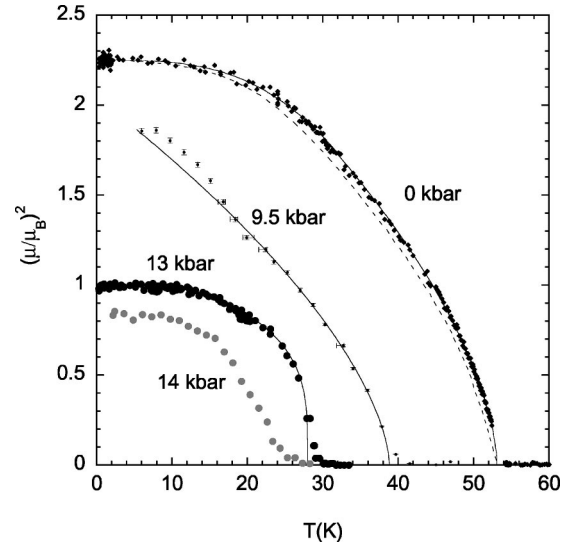


FIG. 8. The diffracted intensity of the magnetic contribution to the $\langle 001 \rangle$ peak as a function of temperature for different pressures. The data have been scaled to give the correct value of M^2 at zero pressure and temperature determined independently by neutron scattering in the absence of the pressure cell. The solid line through the $P=0$ data represents a function $M \propto (1 - T/T_{Curie})^n$ with $n = 0.30$ above 30 K and $M^2 \propto 1 - (T/T_{Curie})^m$ with $m = 3.2$ below 30 K. The line through the data at $P=9.5$ kbar is for the same exponent n . A different, much smaller exponent is, however, required to describe the sharper curvature near T_{Curie} at 13 kbar. The dashed line is the saturation magnetization at $P=0$ determined in a magnetometer.

stronger 002 reflection. At ambient pressure the total ferromagnetic moment M_s measured in a SQUID magnetometer is also shown. To facilitate comparison, M_s has been scaled by a few percent to be equal to the value of M_f at low temperature. The evolution of M_s is then seen to follow closely the evolution of M_f measured by neutron scattering. The small difference is in part due to difficulties in determining the total ferromagnetic moment in the direct magnetization measurements. In these measurements at low temperature, sufficiently strong fields have to be applied to ensure the sample is monodomain. Close to T_{Curie} , however, small fields have to be used to distinguish the zero-field ordered moment from the large linear response.

The relationship between the Curie temperature and saturation magnetization predicted⁴⁰ in the standard SCR (self-consistent renormalization) theory for weak itinerant ferromagnetism is $T_{Curie} \propto M_0^{3/2}$. At 13 kbar the low-temperature moment we observe is $1.0\mu_B/\text{uranium}$ and the critical temperature is 28 K, which can be compared to $1.5\mu_B$ and 53 K at zero pressure. The anomalous temperature dependence of the data at 9.5 kbar below T_x discussed in the next paragraph, however, means that the relationship between T_{Curie} and M_0 for UGe₂ is probably more complicated than the simple theoretical form given above.

At ambient pressure above $T_{Curie}/2$ the temperature dependence of the neutron data fit well a law $M \propto (1 - T/T_{Curie})^\alpha$. The critical exponent $\alpha = 0.30$ is close to the value 0.326, predicted for a three-dimensional Ising magnet.⁴¹ The same

critical exponent also fits the data at 9.5 kbar. However, at low temperature below $T_x \approx 5$ K, the magnetization density shows a positive deviation from this law contrary to the expected saturation of the moment. This suggests that the ferromagnetic component of the order is slightly enhanced below T_x . For the case of a CDW/SDW, the opening of a gap over a section of the Fermi surface would reduce the total density of states and the magnetic fluctuations. Since these fluctuations are responsible for reducing the Curie temperature from the Stoner (mean field) value, their partial suppression could indeed lead to an increase in the ordered moment as observed. It is then at first sight surprising that no clear effect is visible at zero pressure near $T_x = 30$ K. The explanation for this is probably related to the weakening of the anomaly seen in the resistivity discussed earlier. We note, however, that over a wide temperature range and in particular at low temperature the zero-pressure data is well described by $(M/M_0)^2 = 1 - (T/T_0)^n$, with n close to 3 and T_0 only slightly higher than T_{Curie} . This is not consistent with a $(M/M_0) = 1 - (T/T_0)^{3/2}$ dependence at low temperature that would be expected if there was a significant population of noninteracting ungapped spin waves. Further, the exponent is higher than the value $n = 2$ expected for a simple weak itinerant ferromagnet.⁴²

The slope dM/dT at T_{Curie} appears to be substantially higher than given by the Ising model at $P = 13$ kbar. The previous observation of metamagnetic phenomena¹⁵ above P_c suggest that the transition is second order at low pressure but becomes first order at some pressure below P_c . This would explain the observed increase in the slope with pressure near 13 kbar, a vertical slope would be expected when the transition became first order. At still higher pressures dT_{Curie}/dP becomes larger and therefore even a small pressure gradient will cause a smearing of the measured slope dM/dT due to a spread in values of T_{Curie} . A very similar experimental situation pertains for the evolution of $M(T)$ with composition in the series of compounds $\text{UCoAl}_{1-x}\text{Ga}_x$, where the compositional parameter x plays the role of the pressure in UGe_2 ; $x = 0$ corresponds to the high-pressure paramagnetic state and an increasing x to reducing the pressure.⁴³ Compositional disorder would play the role of the small pressure gradient. Interestingly, the analogy extends to the metamagnetic behavior. In both $\text{UCoAl}_{1-x}\text{Ga}_x$ and UGe_2 metamagnetic behavior is found both starting in the paramagnetic state (high pressure or small x) and for a limited range of compositions just within the ferromagnetic state. A similar metamagnetic behavior has also been reported in the series of compounds $\text{Y}_{1-t}\text{Gd}(\text{Co}_{1-x}\text{Al}_x)_2$.⁴⁴ This suggests that the underlying physics of the magnetism is indeed not unique to UGe_2 or to uranium compounds. The disorder due to the random sites of the substituted atoms in these other materials would, however, rule out any possibility of finding spin-triplet superconductivity in those cases.

As well as examining the known nuclear and magnetic peaks that were accessible, we also looked additionally for long-wavelength modulations ($q > 0.002 \text{ \AA}^{-1}$) close to the 001 magnetic peak along the three principal crystal directions. Further scans were made at low temperature and $P = 13$ kbar including a scan along $(1, 1, 0.5 + \delta k)$ to look for

further components of the magnetic structure. No extra peaks were detected at this pressure, or in scans along the crystal axis at $P = 17 \text{ kbar} > P_c$ (the paramagnetic state), or in more extensive scans at low temperature and ambient pressure. The measurements do not, however, rule out the possibility of a change in the magnetic or crystal structure with pressure. A nesting transition need not necessarily give a modulation vector close to a high-symmetry direction and therefore might not be seen in these scans. A study with a Laue camera at ambient pressure and low temperatures provided a more systematic survey of q space. However, again no additional diffraction peaks were detected. The amplitude of any structural or magnetic modulation could, however, be very small, as is the case of the charge density wave in alpha uranium.⁴⁵ A final possibility is that the nesting could concern mainly non- f electrons whereas the neutron data detect the component of the magnetization density principally due to the f electrons and the displacement of the nuclei.

The data taken at 13 kbar extend down to 300 mK, which is below the temperature for which superconductivity occurs (the superconducting transition is complete in the sense that the resistivity is zero up to above 400 mK at this pressure). At these low temperatures the intensity of the magnetic scattering (determined with a sensitivity of 2%) and the width of the magnetic peak showed no detectable temperature dependence. Thus there is no strong modification of the magnetic order on entering the superconducting state. The order of magnitude of the condensation energy of the superconducting state $N_0 T_{\text{sc}}^2$ (N_0 is the density of states at the Fermi energy) should be compared to a much larger energy of order $N_0 T_0^2 (\mu/\mu_B)^2$ for the formation of the ferromagnetic order (T_0 is the Stoner temperature $T_0 > T_{\text{Curie}}$). The anticipated change in the ferromagnetic moment due to the appearance of spin-triplet superconductivity is then expected to be extremely small, at most of order $T_{\text{sc}}/T_{\text{Curie}}$. Finally, we comment on the possibility of observing a modulated structure in the superconducting state. The spontaneous magnetization at zero pressure is $0.19 \text{ T}/\mu_B$ (i.e., for $1.0 \mu_B/\text{uranium}$ at 13 kbar, $\mu_0 M = 0.19 \text{ T}$). This would give a flux-line spacing corresponding to a wave vector of 0.006 \AA^{-1} for a conventional flux-line lattice. The modulation of the magnetic field associated with a conventional flux-line lattice is smaller than $\phi_0/2\pi\lambda_L^2$. The expected modulation of the f -moments is then equal to the susceptibility multiplied by this value. The amplitude of the resulting modulation is thus estimated to be many orders of magnitude too small to be observable relative to the strong ferromagnetic Bragg peak with a conventional diffractometer.

FLUX-FLOW RESISTIVITY

The observation of the zero-resistance state in UGe_2 appears to be particularly sensitive to the magnitude of the applied current. Low critical currents have previously been observed in clean single crystals of other high- κ superconductors ($\kappa = \lambda_L/\xi$, where λ_L is the penetration length and ξ the superconducting coherence length). Typical values of the critical current density J_c (for $B/B_{c2} \approx 0.5$ and $T/T_{\text{sc}} \approx 0.5$) of the order 100 \AA cm^{-2} have been reported^{46,47} for CeRu_2 (κ

=17), while a value of 10 \AA cm^{-2} has been reported⁴⁸ for the nonconventional superconductor UPt₃ ($\kappa=50$). For comparison the value we find for UGe₂ under the same conditions at 11.4 kbar is 0.1 \AA cm^{-2} . The critical current, of course, depends on the concentrations and types of defects. However, for equivalent concentrations of defects, a higher κ tends to favor a lower value of the critical current for the relevant case of weak collective pinning.⁴⁹ This occurs because the decrease with κ of f_p , the maximum force exerted by a single defect, more than compensates a reduction in rigidity of the flux-line lattice. Thus a very small value of J_c could simply indicate a pure sample with a large value of κ . However, it is important to eliminate an alternative explanation, that the low value of J_c is indicative of weak filamentary superconductivity. To this end we performed some voltage versus current measurements at elevated current densities (Fig. 9) in different transverse fields. A linear response was obtained when the current was well above the critical current, with a constant differential resistance, $r = dV/dI$, that at low fields was well below the resistance of the normal state, r_N . For filamentary superconductivity a linear response would not be expected, since the differential resistance would increase with the current as the peak current density exceeded the critical current for successive individual filaments. If all the filaments were similar, the normal-state resistance would be rapidly approached. Our results are instead compatible with the standard theory for a bulk flux-flow resistivity.⁵⁰ The linear differential resistance r increases smoothly with $h = H/H_{c2}$ and approaches r_N at $h = 1$ [Fig. 9(b)]. The concave form of the curve agrees with the predictions of the time-dependent Ginzburg-Landau theory as applied to conventional bulk superconductivity.^{51,52} In this theory $d(r/r_N)/dh \approx 5$ is predicted at $h = 1$, which agrees with our results. At lower field our data also appears to agree with this theory. For comparison, in a recent study of the flux-flow resistivity of the nonconventional superconductor UPt₃,⁵³ an unusual convex curvature of r/r_N versus h was found. In UPt₃ the superconductivity is probably unitary, although still spin triplet.⁵⁴ This is natural since for UPt₃ the magnetic anisotropy constrains the electronic spins to lie in the basal plane of the hexagonal structure. For UGe₂ we have argued that the moments are Ising-like, and are constrained to point along a single crystalline direction. This would suggest that a nonunitary⁵⁵ superconducting state should be formed. In such a state the superconducting gap is different for the majority and minority spin directions. A very small gap for one spin direction might be expected, which would then justify the application of the time-dependent Ginzburg-Landau theory⁵⁰ to low magnetic fields as in the case of a classical gapless superconductor. Further, the penetration length λ_L would be large if the superconducting gap is close to zero over large regions of the Fermi surface. A large value for λ_L is also expected from the large mass renormalization suggested by the large T^2 coefficient in the resistivity near P_x . The large mass renormalization and the large slope of dH_{c2}/dT also indicate a small value for the coherence length ($\xi = 100 \text{ \AA}$) and thus a large value of κ , as suggested by the small values of the critical current.

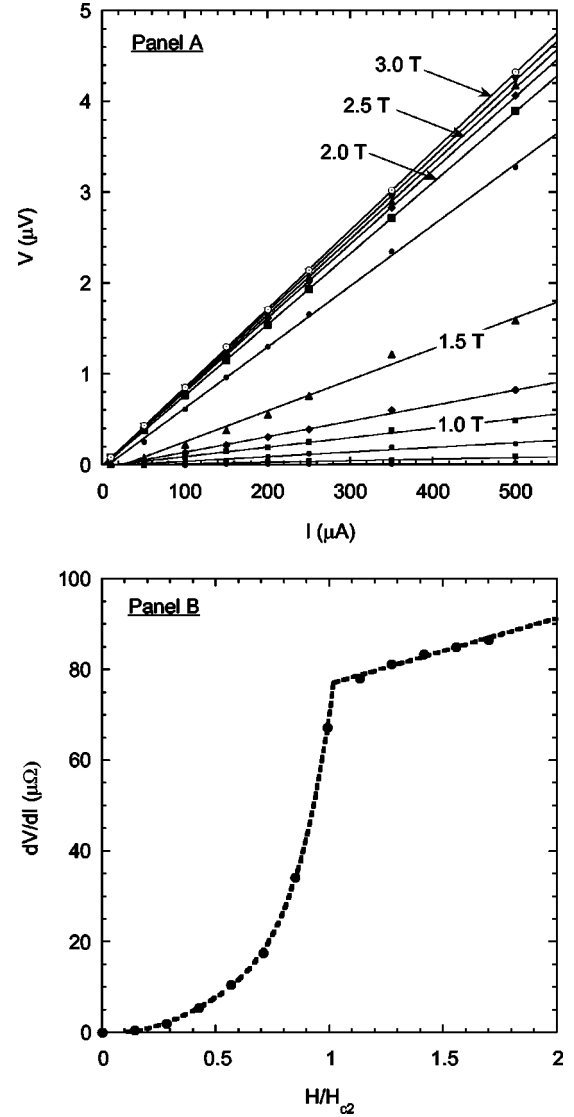


FIG. 9. Panel A shows the ac voltage-current ($V-I$) dependence measured in the superconducting state at 300 mK and a pressure of 11.5 kbar in different applied magnetic fields. The measurements correspond to transverse applied fields increasing from zero in steps of 0.25 T to 3 T (for clarity not all of the curves are labeled). Measurements in zero applied field and at 0.25 T are indistinguishable from the ordinate axis. Panel B shows the linear slopes through these points dV/dI plotted against the field normalized to H_{c2} . The observed behavior strongly resembles that expected for the flux-flow resistivity of a gapless bulk type-II superconductor. The dashed line is to guide the eye.

UPPER CRITICAL FIELD

A further confirmation that the superconductivity is a bulk property is provided by the fact that the upper critical field varies smoothly with angle at pressures away from P_x .⁵⁶ Although we have performed extensive measurements of the upper critical field for all three crystallographic directions at different pressures, we limit our discussion here to the case for the field parallel to the easy axis. The temperature dependence of this critical field measured at three pressures is shown in Fig. 10. The measurements were made with small

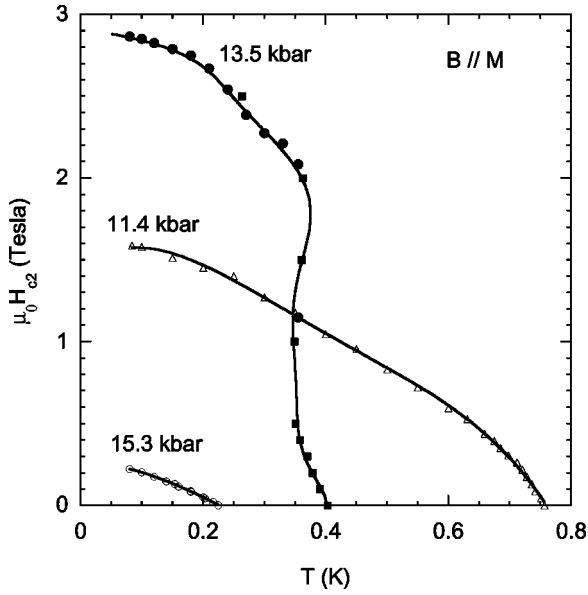


FIG. 10. The upper critical field is shown for applied fields parallel to the a direction (the easy magnetic axis) at three different pressures. The temperature dependence of H_{c2} at 13.5 kbar is highly unusual and is discussed in the main text. At this pressure we have distinguished the points measured by sweeping the field (square symbols) from those measured by sweeping the temperature at constant field (circles). Examples of the measured resistivity curves can be found in Fig. 11. In all the figures the lines serve only to associate the points.

currents and the criteria of $\rho(T, H)/\rho_N = 1/2$ was taken to define H_{c2} . The features we describe below do not depend on the particular choice of these criteria. The first obvious feature of the data is a strong downward curvature of H_{c2} at small fields of the order 0.2 T, particularly visible at 11.4 kbar. This is understandable from the fact that the total field is the sum of the applied field H_{app} and a field due to the magnetization of the sample. The latter depends on the distribution of magnetic domains and is therefore not necessarily homogeneous or directed everywhere parallel to H_{app} . The local magnetization corresponds to 0.19 T per μ_B /uranium and is therefore of the same order of magnitude as the field range over which the strong curvature is seen. The value of $H_{c2}(0)/T_{sc}$ is seen to be rather large and most notably at 13.5 kbar exceeds the so-called paramagnetic limiting field $H_p/T_{sc} = 1.84$ T/K for conventional isotropic superconductivity,^{57,58} although the application of the limit directly to UGe₂ requires careful consideration. The paramagnetic limit is, however, not expected to apply to odd-parity superconductivity when the field is directed along a direction where the total spin of the Cooper pairs can be nonzero. Our results are therefore compatible with the hypothesis of spin-triplet superconductivity, whereas careful discussion would be necessary to reconcile them with a spin-singlet state. For a spin-triplet state another higher limiting field H_l might eventually be reached due to the effect of the field on the nonzero orbital momentum of the Cooper pairs,⁵⁹ $H_l = (m^*/m)H_p$ (where m^*/m is the ratio of the effective electron mass to the bare mass).

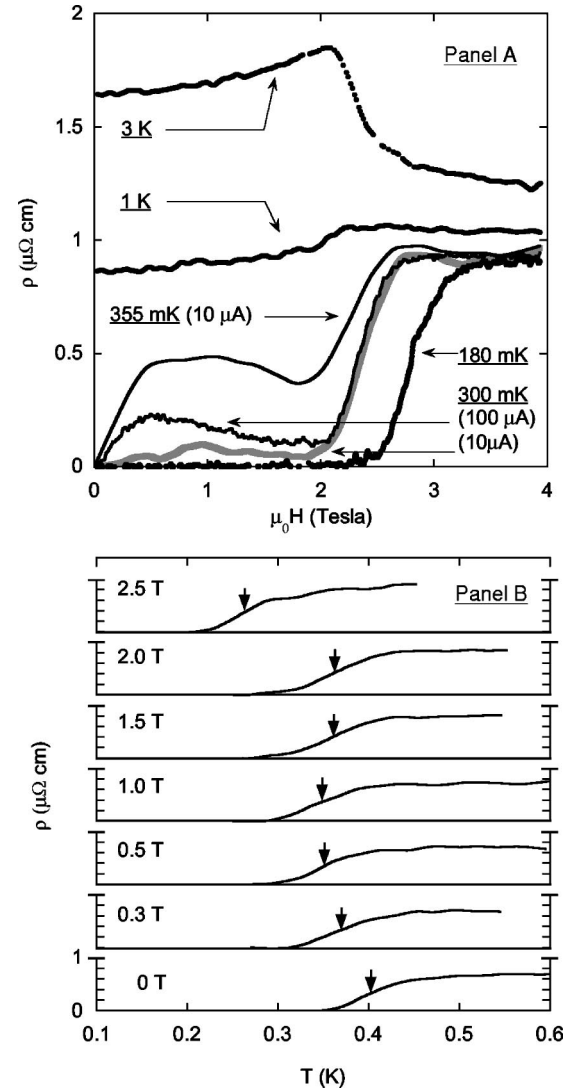


FIG. 11. Panel A shows the resistivity plotted against the applied field at $P = 13.5$ kbar at several temperatures. Both the current and field directions are parallel to the a axis. There is a clear correlation between the upper critical field H_{c2} near T_{sc} in the superconducting state and the field at which there is a transition in the magnetoresistivity at higher temperature (curves at 1 and 3 K). All the data were measured for a current $I = 100 \mu\text{A}$, except for the second trace at 300 mK and the curve at 355 mK, which are for $I = 10 \mu\text{A}$. In panel B representative curves of the resistivity as a function of the temperature at constant field are given. The arrows indicate the positions at which the resistivity is considered to have half its normal-state value.

We now examine the most striking feature of our data, the sharp jump of the upper critical field at 13.5 kbar just below T_{sc} . At this pressure an extrapolation of H_{c2} from below 300 mK in Fig. 10 would suggest a value of T_{sc} closer to the maximum value found for pressures near P_x rather than the value of 400 mK we observe. The resistance data at several temperatures and fields are shown in Fig. 11, along with the curves for the magneto-resistivity at temperatures above T_{sc} . Strikingly, the large value of H_{c2} that occurs just below T_{sc} corresponds to the field at which there is a ‘‘metamagnetic’’

transition in the ferromagnetic state. In our previous discussion we suggested that the applied field inflates and deflates the spin-majority and spin-minority Fermi surfaces and reestablishes the nesting condition that exists below P_x in zero field. If it is the fluctuations associated with this transition that drive the superconductivity, the application of a field at a pressure just above P_x thus also strengthens the superconductivity and this could then explain the near reentrant behavior. Expressed differently, we would say that the coupling constant for the superconductivity depends strongly on the applied field and is enhanced as the nesting condition is approached.

We show in the figure the resistivity against field curves at 300 mK, measured for two values of the current to emphasize that J_c becomes small close to T_{sc} . In our earlier discussion the jump in the residual resistivity at 2 T (visible at 1 K) was related to a reduction in the electronic density of states, possibly due to the appearance of a field-induced CDW/SDW phase. It is not an incomplete transition to superconductivity. Finally, we note that an inhomogeneous superconducting state modulated along the field direction can occur theoretically in a strongly paramagnetic singlet superconductor at high field.^{60,61} Experimental and theoretical investigations to examine the relevance of similar states in a ferromagnetic triplet superconductor and in the presence of a CDW/SDW are left to future work.

CONCLUSIONS

One of the original motivations for our study of UGe₂ was to look for odd-parity spin-triplet superconductivity in the vicinity of the critical pressure P_c , where ferromagnetism disappears. This type of superconductivity mediated by magnetic fluctuations in analogy to the A1-phase⁶² of ³He is predicted to occur generally near and on both sides of a second-order ferromagnetic quantum-critical point.⁸ In general, however, such a state is difficult to observe due to the need to have high enough quality crystals of the appropriate materials. Our initial investigation was focused on pressures just above P_c , where no signature of superconductivity was seen down to 70 mK. An observed metamagnetic behavior¹⁵ above P_c , however, indicated that the magnetic transition was probably first order at pressures just below P_c and therefore the divergence of the fluctuation amplitude, characteristic of a second-order quantum-critical point would no longer be expected. In performing this work we did, however, observe a response in the ac-susceptibility characteristic of superconductivity (a complete diamagnetism in the limit of very small ac fields) at a lower pressure just inside the ferromagnetic state.

The present article provides a more extensive and substantial account of some of the experimental data reported or referred to in Ref. 1, which established the pressure domain over which superconductivity exists. In particular we have provided evidence that ferromagnetism and bulk superconductivity actually do physically coexist, in the sense that both are bulk properties. To this end we have discussed our measurements of the flux-flow resistivity that appear to be consistent with a bulk superconducting state. Such a conclu-

sion might have otherwise been questioned in view of the small values found for the superconducting critical current. We have also established that the ferromagnetic component of the order is still large (of the order $1\mu_B/\text{uranium}$) at a pressure and temperature where superconductivity is found.

Our continued investigation of the phase diagram has revealed a strong correlation between a transition at T_x within the ferromagnetic state and the appearance of superconductivity; the maximum transition temperature for superconductivity occurs near to the pressure P_x where T_x vanishes. In this light, it is interesting to ask whether P_x might correspond to a second-order quantum-critical point for an as yet unidentified order parameter in lieu of the first-order transition at P_c . This question remains open, although we point out that any potential experimental determination of the order of this transition based on detecting hysteresis is less than straightforward. This is because the domain structure of the underlying ferromagnetic state could itself give rise to some irreversible behavior. In agreement with previous work we found that the enhancement of the temperature dependence of the resistivity at P_x is slightly more significant than at P_c . This suggests that the low energy fluctuations associated with the transition at P_x might, regardless of the order of the transition, be at least as important as those associated with P_c and therefore could play a significant role in forming or enhancing the superconductivity. A comparison with the case of alpha uranium and the calculated band structure for UGe₂ suggest that the transition at P_x might be related to a Fermi-surface nesting and a tendency toward the formation of a CDW/SDW. The formation of such a state would depend on the geometry of particular sheets of the Fermi-surface. This geometry could change significantly with the magnitude of the ferromagnetic ordered moment, due to the change in population of the majority and minority spin bands. It is then a natural possibility that the CDW/SDW transition is confined to the ferromagnetic phase, at least for low applied fields. The above scenario is also supported by our observation that there is a metamagnetic transition within the ferromagnetic state at pressures just above P_x . It also explains qualitatively the observed changes in the residual resistivity, and a small change in the ferromagnetic component of the order at T_x noted in our neutron scattering study. However, our efforts to detect any CDW/SDW modulation by neutron scattering have not been successful.

Irrespective of the origin of the transition at P_x , the fact that it can be induced by field at higher pressure provides a qualitative explanation for a near reentrant behavior of the superconductivity with field, that we have observed at $P = 13.5$ kbar. This emphasizes that there is a close relationship between the superconductivity and the proximity to this transition.

Future work is clearly required to look more carefully for small modulations of the structure or spin density and to look for low-energy modes related to P_x . If a CDW/SDW is found to occur only below P_x , we are indeed dealing with the coexistence of ferromagnetism and superconductivity between P_x and P_c . Below P_x the magnetic structure might turn out to be more accurately described as ferrimagnetic. The eventual identification of the nature of the transition at

P_x should also clarify whether the pairing interaction is predominantly spin based, phononic or due to the combined action of both mechanisms.

ACKNOWLEDGMENTS

We are grateful to S. Tajima *et al.* for showing us their recent band structure calculations for the Cmmm structure.

We also thank F. Bourdarot, B. Grenier, G. McIntyre, F. Thomas, S. Pujol, and L. Melesi for help in performing the neutron scattering measurements. It is also a pleasure to acknowledge discussions with Profs. K. Miyake, G. G. Lonzarich, K. Machida, P. Canfield, V. Mineev, N. Bernhoeft, A. Buzdin, P. Littlewood, J. P. Brison, R. Ballou, and our collaborators from the University of Cambridge low temperature group, S. Saxena, P. Agarwal, K. Ahilan, M. Grösche, and S. Julian.

- ¹S. S. Saxena, P. Agarwal, K. Ahilan, F. M. Grosche, R. K. W. Hasselwimmer, M. J. Steiner, E. Pugh, I. R. Walker, S. R. Julian, P. Monthoux, G. G. Lonzarich, A. Huxley, I. Sheikin, D. Braithwaite, and J. Flouquet, *Nature (London)* **406**, 587 (2000).
- ²D. E. Moncton, D. B. McWahn, P. H. Schmidt, G. Shirane, W. Thomlinson, M. B. Maple, H. B. MacKay, L. D. Woolf, Z. Fisk, and D. C. Johnston, *Phys. Rev. Lett.* **45**, 2060 (1980).
- ³W. A. Fertig, D. C. Johnston, E. DeLong, R. W. McCallum, M. B. Maple, and B. T. Matthias, *Phys. Rev. Lett.* **38**, 987 (1977).
- ⁴M. Ishikawa and Ø. Fischer, *Solid State Commun.* **23**, 37 (1977).
- ⁵P. C. Canfield, S. L. Bud'ko, and B. K. Cho, *Physica C* **262**, 249 (1996).
- ⁶T. Hermamsdörfer, S. Pehmann, M. Seibold, and F. Pobell, *J. Low Temp. Phys.* **110**, 405 (1998).
- ⁷C. Bernhard, J. L. Tallon, Ch. Niedermayer, Th. Blasius, A. Golnik, E. Brücher, R. K. Kremer, D. R. Noakes, C. E. Sronach, and E. J. Ansaldo, *Phys. Rev. B* **59**, 14 099 (1999).
- ⁸D. Fay and J. Appel, *Phys. Rev. B* **22**, 3173 (1980).
- ⁹G. G. Lonzarich, in *Electron: A Centenary Volume*, edited by M. Springford (Cambridge University Press, Cambridge, 1999), p. 109.
- ¹⁰V. Sechovsky and L. Havela, in *Handbook of Magnetic Materials*, edited by K. H. J. Buschow (North-Holland, Amsterdam, 1998), Vol. 11, p. 1.
- ¹¹K. Oikawa, T. Kamiyama, H. Asano, Y. Onuki, and M. Kohgi, *J. Phys. Soc. Jpn.* **65**, 3229 (1996).
- ¹²P. Boulet, A. Daoudi, M. Potel, H. Noël, G. M. Gross, G. André, and F. Bourée, *J. Alloys Compd.* **247**, 104 (1997).
- ¹³P. Söderland, O. Eroksson, J. Börje, J. M. Wills, and A. M. Borning, *Nature (London)* **374**, 524 (1995).
- ¹⁴J. Akella, S. Weir, J. M. Wills, and P. Söderland, *J. Phys.: Condens. Matter* **9**, L549 (1997).
- ¹⁵A. Huxley, I. Sheikin, and D. Braithwaite, *Physica B* **284-288**, 1277 (2000).
- ¹⁶L. Fast, O. Eriksson, B. Johansson, J. M. Wills, G. Straub, H. Roeder, and L. Nordström, *Phys. Rev. Lett.* **81**, 2978 (1998).
- ¹⁷J. C. Mermeggi, R. Currat, A. Bouvet, and G. H. Lander, *Physica B* **263-264**, 624 (1999).
- ¹⁸H. Yamagami and A. Hasagawa, *Physica B* **186-188**, 182 (1993).
- ¹⁹S. Tajima, H. Yamagami, and N. Hamada, *J. Phys. Soc. Jpn.* (to be published).
- ²⁰H. G. Smith, N. Wakabayashi, R. M. Nicklow, G. H. Lander, E. S. Fisher, and W. B. Daniels, *Proceedings of the Conference on Superconductivity in d and f-band Metals, Karlsruhe, Germany, 1982*, edited by W. Buckel and W. Weber (KfK, Karlsruhe, 1982), p. 463.
- ²¹H. H. Hill, in *Plutonium and Other Actinides*, edited by W. N. Miner (A.I.M.E., New York, 1970), p. 2.
- ²²P. Mohn and G. Hilscher, *Phys. Rev. B* **40**, 9126 (1989).
- ²³P. R. Rhodes and E. P. Wohlfarth, *Proc. R. Soc. London* **273**, 247 (1963).
- ²⁴E. P. Wohlfarth, *J. Magn. Magn. Mater.* **7**, 113 (1978).
- ²⁵Y. Onuki, I. Ukon, S. Won Yun, I. Umehara, K. Satoh, T. Fukuhara, H. Sato, S. Takayanagi, M. Shikama, and A. Ochiai, *J. Phys. Soc. Jpn.* **61**, 293 (1992).
- ²⁶A. J. Millis, S. Sachdev, and C. M. Varma, *Phys. Rev. B* **37**, 4975 (1988).
- ²⁷S. W. Yun, K. Satoh, Y. Fujimah, I. Umehara, Y. Onuki, S. Takayanagi, H. Aoki, S. Uji, and T. Shimizu, *Physica B* **186-188**, 129 (1993).
- ²⁸G. Oomi, T. Kagayama, and Y. Onuki, *J. Alloys Compd.* **271-273**, 482 (1998).
- ²⁹G. Oomi, K. Nishimura, Y. Onuki, and S. W. Yun, *Physica B* **186-188**, 758 (1993).
- ³⁰H. Nakotte, F. R. de Boer, L. Havela, P. Svoboda, V. Sechovsky, Y. Kergadallan, J. C. Spirlet, and J. Rebizant, *J. Appl. Phys.* **73**, 6554 (1993).
- ³¹W. Kohn, *Phys. Rev. Lett.* **2**, 393 (1959).
- ³²H. Takahashi, N. Mōri, Y. Onuki, and S. W. Yun, *Physica B* **186-188**, 772 (1993).
- ³³S. Saxena, Ph.D. thesis, University of Cambridge, 1998.
- ³⁴W. L. McMillan, *Phys. Rev. B* **16**, 643 (1977).
- ³⁵P. B. Littlewood and V. Heine, *J. Phys. C* **14**, 2943 (1981).
- ³⁶P. M. Marcus, S. L. Qiu, and V. L. Moruzzi, *J. Phys. C* **10**, 6541 (1998).
- ³⁷N. Kernavanois, B. Grenier, A. Huxley, E. Ressouche, J. P. Sanchez, and J. Flouquet (unpublished).
- ³⁸R. C. Maglic, G. H. Lander, M. H. Mueller, and R. Kleb, *Phys. Rev. B* **17**, 308 (1978).
- ³⁹M. S. S. Brooks and B. Johansson, in *Handbook of Magnetic Materials*, edited by K. H. J. Buschow (North-Holland, Amsterdam, 1993), Vol. 7, p. 139.
- ⁴⁰T. Moriya, *Spin Fluctuations in Itinerant Electron Magnetism* (Springer-Verlag, Berlin, 1985).
- ⁴¹J. C. LeGuillou and J. Zinn-Justin, *J. Phys. (France) Lett.* **46**, L137 (1985).
- ⁴²G. G. Lonzarich and L. Taillefer, *J. Phys. C* **18**, 4339 (1985).
- ⁴³A. V. Andreev, *J. Alloys Compd.* **269**, 34 (1998).
- ⁴⁴R. Ballou, Z. M. Gamishidze, R. Lemaire, R. Z. Levitin, A. S. Markosyan, and V. V. Snegirev, *Zh. Eksp. Teor. Fiz.* **102**, 1936 (1992) [*Sov. Phys. JETP* **75**, 1041 (1992)].

- ⁴⁵G. H. Lander, E. S. Fisher, and S. D. Bader, *Adv. Phys.* **43**, 1 (1994).
- ⁴⁶M. Hedo, Y. Kobayashi, Y. Inada, E. Yamamoto, Y. Haga, J. Suzuki, N. Metoki, Y. Onuki, H. Sugawara, H. Sato, K. Tenya, T. Tayama, H. Amitsuka, and T. Sakakibara, *Physica B* **259-261**, 688 (1999).
- ⁴⁷A. Huxley, N. H. van Dijk, D. McK. Paul, R. Cubitt, and P. Lejay, *Physica B* **259-261**, 696 (1999).
- ⁴⁸S. Kambe, A. Huxley, P. Rodière, C. Paulsen, and J. Flouquet, *Physica B* **259-261**, 670 (1999).
- ⁴⁹A. I. Larkin and Y. N. Ovchinnikov, *J. Low Temp. Phys.* **34**, 409 (1979).
- ⁵⁰C. Hu and R. S. Thompson, *Phys. Rev. B* **6**, 110 (1971).
- ⁵¹K. Maki, *Prog. Theor. Phys.* **41**, 902 (1969).
- ⁵²K. Maki and A. Houghton, *Phys. Rev. B* **4**, 847 (1971).
- ⁵³S. Kambe, A. Huxley, P. Rodière, and J. Flouquet, *Phys. Rev. Lett.* **83**, 1842 (1999).
- ⁵⁴J. A. Sauls, *Adv. Phys.* **43**, 113 (1994).
- ⁵⁵T. Ohmi and K. Machida, *Phys. Rev. Lett.* **71**, 625 (1993).
- ⁵⁶I. Sheikin, A. Huxley, D. Braithwaite, and J. Flouquet (unpublished).
- ⁵⁷A. M. Clogston, *Phys. Rev. Lett.* **9**, 266 (1962).
- ⁵⁸B. S. Chandrasekhar, *Appl. Phys. Lett.* **1**, 7 (1962).
- ⁵⁹I. A. Luk'yanchuk and V. P. Mineev, *Pis'ma Zh. Eksp. Teor. Fiz.* **44**, 183 (1986) [*JETP Lett.* **44**, 233 (1986)].
- ⁶⁰P. Fulde and R. Ferrel, *Phys. Rev.* **135**, 550 (1964).
- ⁶¹A. I. Larkin and Y. N. Ovchinnikov, *Zh. Eksp. Teor. Fiz.* **47**, 1136 (1964) [*Sov. Phys. JETP* **20**, 762 (1965)].
- ⁶²K. Levin, *Phys. Rev. Lett.* **34**, 1002 (1975).